

# On boundary conditions for the diffusion equation in room-acoustic prediction: Theory, simulations, and experiments<sup>a)</sup>

Yun Jing and Ning Xiang<sup>b)</sup>

Graduate Program in Architectural Acoustics, School of Architecture, Rensselaer Polytechnic Institute, Troy, New York 12180, USA

(Received 3 July 2007; revised 12 October 2007; accepted 12 October 2007)

This paper proposes a modified boundary condition to improve the room-acoustic prediction accuracy of a diffusion equation model. Previous boundary conditions for the diffusion equation model have certain limitations which restrict its application to a certain number of room types. The boundary condition employing the Sabine absorption coefficient [V. Valeau *et al.*, *J. Acoust. Soc. Am.* **119**, 1504–1513 (2006)] cannot predict the sound field well when the absorption coefficient is high, while the boundary condition employing the Eyring absorption coefficient [Y. Jing and N. Xiang, *J. Acoust. Soc. Am.* **121**, 3284–3287 (2007); A. Billon *et al.*, *Appl. Acoust.* **69**, (2008)] has a singularity whenever any surface material has an absorption coefficient of 1.0. The modified boundary condition is derived based on an analogy between sound propagation and light propagation. Simulated and experimental data are compared to verify the modified boundary condition in terms of room-acoustic parameter prediction. The results of this comparison suggest that the modified boundary condition is valid for a range of absorption coefficient values and successfully eliminates the singularity problem. © 2008 Acoustical Society of America.

[DOI: 10.1121/1.2805618]

PACS number(s): 43.55.Br, 43.55.Ka [EJS]

Pages: 145–153

## I. INTRODUCTION

Room-acoustic predictions have been actively researched in the area of architectural acoustics for decades. A diffusion equation-based method has recently drawn attention in this field, partially due to its ability to combine accuracy and efficiency. The purpose of this work is to present a modified boundary condition for diffusion equation-based room-acoustics prediction.

In 1969, Ollendorff<sup>1</sup> first proposed the diffusion model to describe sound fields in enclosures. Later, based on an analogy between sound propagation in rooms with diffusely reflecting walls and particle propagation in a diffusing fluid,<sup>2</sup> Picaut<sup>3</sup> and his co-workers<sup>4–8</sup> demonstrated this diffusion model and extended its application to a variety of enclosure types, including elongated enclosures such as street canyons, single-volume enclosures, fitted rooms, and coupled-volume rooms. For room-acoustics modeling, Valeau *et al.*<sup>5</sup> provide a generalization of the diffusion model that includes two boundary conditions. These studies<sup>3–8</sup> have shown that the diffusion model is computationally efficient compared to the geometrical-acoustics model. The diffusion model also provides more satisfactory results than does statistical room-acoustics theory since it is capable of modeling the nonuniformity of sound fields in enclosures of a wide variety of shapes. However, the diffusion model has been found to be suitable only for use with low absorption coefficients.<sup>5–7</sup> Most recently, another boundary condition exploiting the Ey-

ring absorption coefficient was proposed independently by Jing and Xiang<sup>9</sup> and Billon *et al.*,<sup>10</sup> and was shown to be able to improve the accuracy of the diffusion model when the absorption coefficient of room surfaces is high. The use of the Eyring absorption coefficient is also justified theoretically in this paper.

In this paper, a modified boundary condition is derived from a boundary condition used in solving analogous optical diffusion problems.<sup>11</sup> Incorporating the modified boundary condition in the room-acoustic diffusion equation, this work compares the diffusion models associated with various boundary conditions with a geometrical-acoustic model as well as experimental results obtained from a physical scale model. Predicted reverberation times (RTs) and sound pressure levels (SPLs) are calculated for cubic rooms with both uniformly and nonuniformly distributed absorbing surfaces. For a flat, long room, the geometrical-acoustics model is used for the comparison of the SPL distribution. Acoustical measurements are conducted in a scale-model flat room to validate the modified boundary condition in terms of the predicted SPLs and the RTs.

This paper is structured as follows: Sec. II presents the diffusion equation model for room-acoustic prediction including the interior equation and different boundary conditions. Section III discusses simulation results obtained using the diffusion equation model with different boundary conditions, as well as those obtained using the geometrical-acoustic model. Section IV describes the scale model experiments, and compares the acoustical measurement results with the diffusion equation model for various boundary conditions. Section V concludes the paper.

<sup>a)</sup> Aspects of this work have been presented at the 153rd meeting of the Acoustical Society of America [*J. Acoust. Soc. Am.* **121**, 3174 (A) (2007)].

<sup>b)</sup> Author to whom correspondence should be addressed. Electronic mail: xiangn@rpi.edu

## II. DIFFUSION EQUATION MODEL FOR ROOM-ACOUSTIC PREDICTION

### A. Interior diffusion equation

This section begins with a review of the analogy drawn by Picaut *et al.*<sup>3</sup> between sound propagation in rooms with diffusely reflecting boundaries and gas particle propagation in a diffusing fluid. The motion of a sound particle<sup>12</sup> in a room is equivalent to the movement of a particle in a gas, assuming that there are numerous spherical scattering objects<sup>2</sup> in the volume having scattering cross section  $Q_s$  and absorption cross section  $Q_a$ . Furthermore, in order to respect the same surface distribution between the enclosure and the diffusing fluid, the scattering objects should have mean free path length  $4V/S$ , (for volume  $V$  and interior surface area  $S$  of the enclosure under investigation), which is consistent with classical room-acoustic theory when the walls are considered diffusely reflecting. The scattering objects take the place of the walls and reflect the sound diffusely in the volume. In this case, the sound energy flow vector  $\mathbf{J}$  caused by the gradient of the sound energy density  $w$ , in the room under investigation at position  $\mathbf{r}$  and time  $t$ , can be expressed according to Fick's law as<sup>2,3</sup>

$$\mathbf{J}(\mathbf{r}, t) = -D \text{grad } w(\mathbf{r}, t), \quad (1)$$

with diffusion coefficient  $D$

$$D = \lambda c/3, \quad (2)$$

where  $c$  is the speed of sound and  $\lambda = 4V/S$  is the mean free path of the enclosure under investigation. Here we assume that the rate of change involved in diffusion is slow and the walls are diffusely reflecting. The sound energy density  $w$ , in a region (domain  $V$ ) excluding sound sources, changes per unit time as

$$\frac{\partial w(\mathbf{r}, t)}{\partial t} = -\text{div } \mathbf{J}(\mathbf{r}, t) = D \nabla^2 w(\mathbf{r}, t). \quad (3)$$

In the case of a spatially distributed omni-directional sound source within a region with time-dependent energy density  $q(\mathbf{r}, t)$  Eq. (3) is replaced by

$$\frac{\partial w(\mathbf{r}, t)}{\partial t} = q(\mathbf{r}, t) + D \nabla^2 w(\mathbf{r}, t), \quad (4)$$

while absorption at the room boundaries leads to energy loss per unit volume ( $\sigma w$ ) in the absence of sound sources, so the energy balance can be written as

$$\begin{aligned} \frac{\partial w(\mathbf{r}, t)}{\partial t} &= D \nabla^2 w(\mathbf{r}, t) - \sigma w(\mathbf{r}, t) \\ &= D \nabla^2 w(\mathbf{r}, t) - Q_a n_t c w(\mathbf{r}, t), \end{aligned} \quad (5)$$

where  $\sigma = \bar{\alpha} c / \lambda = Q_a n_t c$ , with  $\bar{\alpha}$  being the mean room-surface absorption coefficient according to Ref. 3. The validity of Eq. (5) will be discussed in Sec. II B.

Taking into account both absorption of room boundaries and sound source excitations in the room under investigation, the combination of Eqs. (4) and (5) yields the diffusion equation

$$\frac{\partial w(\mathbf{r}, t)}{\partial t} - D \nabla^2 w(\mathbf{r}, t) + \sigma w(\mathbf{r}, t) = q(\mathbf{r}, t) \quad \text{in } V. \quad (6)$$

It is also possible to include air absorption inside the enclosure using the diffusion equation<sup>13</sup>

$$\begin{aligned} \frac{\partial w(\mathbf{r}, t)}{\partial t} - D \nabla^2 w(\mathbf{r}, t) + \sigma w(\mathbf{r}, t) + m c w(\mathbf{r}, t) \\ = q(\mathbf{r}, t) \quad \text{in } V, \end{aligned} \quad (7)$$

where  $m$  is the coefficient of air absorption. All absorption coefficients are frequency dependent, so the frequency dependence of sound energy density of enclosures may be included in the diffusion equation model.<sup>5</sup> For simplicity, however, the following discussion will not consider the air absorption.

### B. Boundary conditions

#### 1. Previous boundary conditions

In an enclosure bounded by surfaces (denoted by  $S$ ), the boundary condition

$$\mathbf{J}(\mathbf{r}, t) \cdot \mathbf{n} = -D w(\mathbf{r}, t) \cdot \mathbf{n} = 0, \quad \text{on } S \quad (8)$$

states that sound energy cannot escape from the room boundaries, with  $\mathbf{n}$  denoting the surface outgoing normal. Equation (8) is the so-called *homogeneous Neumann boundary condition*.<sup>2,5</sup> The diffusion equation model with the homogeneous Neumann boundary condition considers only an overall mean absorption coefficient  $\bar{\alpha}$  of the enclosure under investigation. Furthermore, it assumes that the absorption occurs in the volume rather than on the room surfaces, which is nonphysical for the current application. Therefore, this boundary condition, mentioned here for completeness, will not be considered in the following investigations.

The boundary condition<sup>2,5</sup>

$$\mathbf{J}(\mathbf{r}, t) \cdot \mathbf{n} = -D w(\mathbf{r}, t) \cdot \mathbf{n} = A_X c w(\mathbf{r}, t), \quad \text{on } S, \quad (9)$$

allows energy exchanges on the boundaries  $S$ , where  $A_X$  is an exchange coefficient denoted in the following as the *absorption factor*. This boundary condition is established to include the absorption at the walls: The local differential equation in Eq. (6) then needs to be modified to remove the absorption term  $\sigma w(\mathbf{r}, t)$  (the following boundary conditions all require that the absorption term in the interior equation drop out), while the term must be introduced into Eq. (9) to account for energy exchanges on the boundaries.<sup>5</sup>

Assuming the sound energy density is uniform in a proportionate room while supposing that the energy density only varies along the long dimension in a disproportionate room [5], the absorption factor can be expressed as

$$A_X = A_S = \frac{\alpha}{4}, \quad (10)$$

where  $\alpha$  is the absorption coefficient of the wall under consideration. The subscript  $S$  of  $A_S$  is used to denote Sabine absorption. Equation (10) implies the Sabine absorption is assigned to the absorption factor  $A_X$ . The resulting system of equations is formulated as

$$\frac{\partial w(\mathbf{r},t)}{\partial t} - D\nabla^2 w(\mathbf{r},t) = q(\mathbf{r},t) \quad \text{in } V, \quad (11)$$

$$D\frac{\partial w(\mathbf{r},t)}{\partial n} + cA_X w(\mathbf{r},t) = 0 \quad \text{on } S, \quad (12)$$

which describe the diffusion equation model [Eq. (11)] with *mixed boundary conditions* [Eq. (12)] for more general situations. The absorption factor  $A_X$  assumes different expressions with different subscript  $X$  as elaborated in the following. It will then be possible to assign different absorption coefficients to each of the individual walls.

The diffusion equation model with this boundary condition is, however, found to be accurate only for modeling rooms with low absorption.<sup>5-7</sup> To improve the accuracy of the mixed boundary condition associated with high absorption, a new boundary condition was conceived independently by these authors<sup>9</sup> and Billon *et al.*<sup>10</sup> It simply replaces the Sabine absorption coefficient in the absorption factor by the Eyring absorption coefficient

$$A_X = A_E = \frac{-\log(1 - \alpha)}{4} \quad (13)$$

to account for high wall absorption in the system of equations in Eqs. (11) and (12).

A justification of the replacement of Eyring absorption coefficient is detailed here. Under the assumption that there are scattering objects in the enclosure, the number  $dN$  of phonons absorbed by the scattering objects, between the points  $x$  and  $x+dx$  along the path of the beam, should be equal to the product of  $N$ , the number of phonons penetrating to depth  $x$ ,  $n_t$ , the number of scattering objects per unit volume and the absorption cross section  $Q_a$ <sup>2</sup>

$$dN/dx = -Nn_tQ_a, \quad (14)$$

where the negative sign indicates the reduction of the phonon due to absorption. Then, a simple integral over  $\lambda$  (the mean free path length) gives

$$N' = N \exp(-n_tQ_a\lambda), \quad (15)$$

where  $N'$  is the number of phonons after penetrating to depth  $\lambda$ .

In room acoustics, the phonon number is reduced after each wall collision according to the absorption coefficient of the wall, which leads to

$$N' = N(1 - \bar{\alpha}), \quad (16)$$

where  $\bar{\alpha}$  is the mean room-surface absorption coefficient. The combination of Eq. (15) and Eq. (16) yields (see also Ref. 14)

$$-\ln(1 - \bar{\alpha}) = n_tQ_a\lambda. \quad (17)$$

A substituting of Eq. (17) into Eq. (5) yields a diffusion equation which is similar to Eq. (5), but with  $\sigma = -\ln(1 - \bar{\alpha})c/\lambda$ . Finally, the Eyring absorption coefficient is applied to each boundary by using an exchange coefficient,<sup>5,9</sup> which gives the boundary condition, i.e., Eq. (12) along with Eq. (13).

Accordingly, the diffusion equation model with the Sabine coefficient in the absorption factor ( $A_X = A_S$ ) is denoted *diffusion-Sabine* model in the following while the model which utilizes the one with the Eyring coefficient ( $A_X = A_E$ ) is denoted *diffusion-Eyring* model.<sup>10</sup> Although the simulation results suggest that the diffusion-Eyring model can improve the accuracy of the diffusion-Sabine model to a certain extent, particularly for cases of high absorption,<sup>9,10</sup> application of this model requires caution as the absorption coefficient  $\alpha \rightarrow 1.0$ . As discussed in the following, the absorption factor  $A_E$  will become singular (infinite) in this case, which is problematic.

## 2. Modified boundary condition

This section presents a modified boundary condition with theoretical justification. The derivation of this boundary condition relies heavily on a well established boundary for light diffusion in media.<sup>11</sup> The modified boundary condition remedies weaknesses in the original diffusion-Sabine model under high absorption and eliminates the singularity of the diffusion-Eyring model. In the following, the diffusion equation model with the modified boundary condition is denoted *modified diffusion model*.

The statement of Picaut *et al.*,<sup>3</sup> which introduces the diffusion interior equation, describes an infinite scattering medium.<sup>5</sup> To bound the scattering medium, the boundary, on the one hand, absorbs a portion of the sound energy at a given absorption coefficient on the corresponding wall. On the other hand, since the boundary is not considered as the wall but artificially imposed to bound the energy, it can be considered to be completely smooth and to reflect specularly the other portion of the sound energy to prevent this portion from leaving the volume. Similar to the previous boundary conditions, different absorption coefficients could be assigned to individual boundaries.

Based on a similar boundary condition in light diffusion, the derivation of the modified boundary condition is presented. Emphasis is given to differences from optical diffusion, and to an explicit formulation of the acoustic boundary condition.

A partial-current boundary condition<sup>11</sup> in light diffusion describes the scenario in which a portion of the energy will be specularly reflected back into the scattering medium when the refractive indices of the strongly scattering medium differ substantially from those of the bounding transparent medium, while the other portion will be refracted and leave the scattering medium.

This boundary condition can be expressed using an optical term fluence rate  $\phi$  in unit  $\text{W m}^{-2}$ .<sup>11</sup> Because sound intensity has the same unit, in the following room-acoustic discussion, notation  $\phi$  represents sound intensity. The relationship between the sound intensity and the sound energy density can be expressed as,<sup>15</sup>

$$\phi(\mathbf{r},t) = c\mathbf{n}'w(\mathbf{r},t), \quad (18)$$

where  $\mathbf{n}'$  is the direction of energy propagation.

Furthermore, the boundary condition is written as

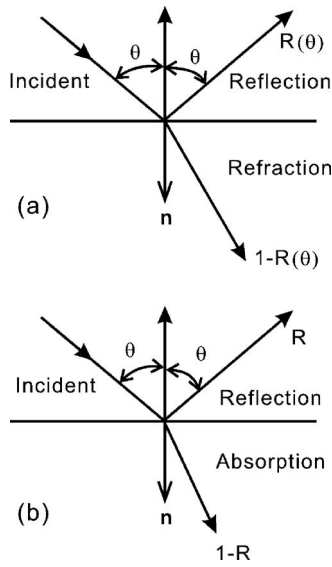


FIG. 1. (a) Light reflection and refraction on a boundary. (b) Sound reflection and absorption on a boundary.

$$\phi(\mathbf{r}, t) = \frac{1 + R_i}{1 - R_\phi} 2\mathbf{J}(\mathbf{r}, t) \cdot \mathbf{n} \quad \text{on } S, \quad (19)$$

where

$$R_\phi = \int_0^{\pi/2} 2 \sin \theta \cos \theta R(\theta) d\theta, \quad (20)$$

$$R_j = \int_0^{\pi/2} 3 \sin \theta \cos^2 \theta R(\theta) d\theta, \quad (21)$$

$$\mathbf{J}(\mathbf{r}, t) \cdot \mathbf{n} = -D' \frac{\partial \phi(\mathbf{r}, t)}{\partial n}, \quad (22)$$

with  $D' = \lambda/3$  being one third of the mean free path length in the medium. Figure 1a schematically illustrates the boundary condition.  $R(\theta)$  is the probability of the light being reflected, also so-called Fresnel reflection coefficient which is a function of the angle of incidence  $\theta$ ,<sup>11</sup>  $\mathbf{n}$  is the outward-drawn normal to the boundary.  $\mathbf{J}$  is the energy flow as explained earlier [see Sec. II A].

The same boundary condition may also be applied to room acoustics since the room-acoustic diffusion equation is essentially the same as the light diffusion equation, and the specular reflection is also desired for the modified acoustic boundary condition proposed in this paper. However, some significant differences should be noted: (1) In the light diffusion boundary condition, the light refracts at the boundary, while in room-acoustics boundary condition, the sound energy is usually considered to be absorbed at the boundary. Nevertheless, since the focus in the current application is on the energy inside the volume, this work disregards the way of sound transmissions beyond the boundary. (2) In room acoustics, the reflectivity  $R$  which represents the probability that the sound will be reflected (energy-based reflectivity) can be expressed using the absorption coefficient as  $1 - \alpha$ , so that it is completely independent of incident angle. (Figure 1b illustrates this concept.) Thus,

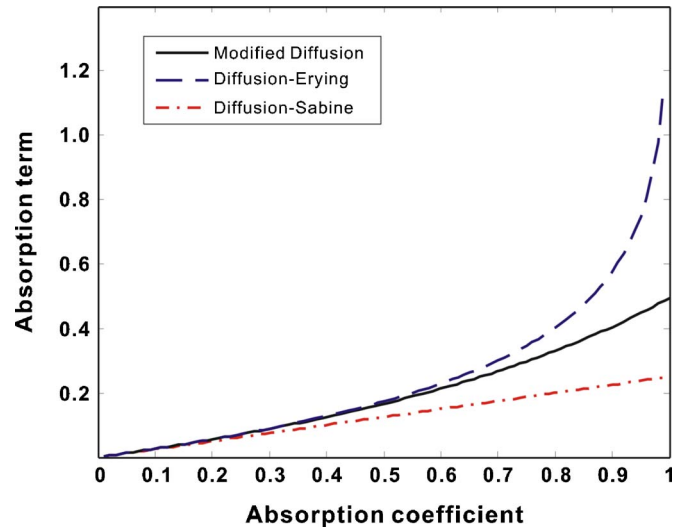


FIG. 2. (Color online). Comparison of the absorption terms of the diffusion-Sabine, diffusion-Eyring, and modified diffusion models versus absorption coefficient.

$$R_\phi = (1 - \alpha) \int_0^{\pi/2} 2 \sin \theta \cos \theta d\theta = 1 - \alpha, \quad (23)$$

$$R_j = (1 - \alpha) \int_0^{\pi/2} 3 \sin \theta \cos^2 \theta d\theta = 1 - \alpha, \quad (24)$$

A substitution of Eqs. (18) and (22)–(24) into (19) yields

$$cw(\mathbf{r}, t) = -\frac{2 - \alpha}{\alpha} 2D \frac{\partial w(\mathbf{r}, t)}{\partial n} \quad \text{on } S, \quad (25)$$

where  $D = \lambda c/3$ , leading to the modified boundary condition

$$D \frac{\partial w(\mathbf{r}, t)}{\partial n} + \frac{c\alpha}{2(2 - \alpha)} w(\mathbf{r}, t) = 0 \quad \text{on } S. \quad (26)$$

A comparison of the boundary conditions of the diffusion-Sabine and diffusion-Eyring models reveals that the only difference between them is the absorption factor associated with absorption coefficient  $\alpha$ ,

$$A_X = A_M = \frac{\alpha}{2(2 - \alpha)}. \quad (27)$$

In order to enable a direct comparison of these boundary conditions, Fig. 2 illustrates the three absorption factors in Eqs. (10), (13), and (27) when varying the absorption coefficient. When the absorption coefficient is lower than 0.2, the difference between the absorption factors  $A_S, A_E, A_M$  is negligible. With increasing absorption coefficient but below 0.6, the difference between absorption term  $A_E$  and  $A_M$  is still negligible, while the absorption term  $A_S$  differs quite significantly from the other two. As the absorption coefficient increases further, the discrepancy between  $A_E$  and  $A_M$  is considerable, warranting in-depth investigation. This behavior is easily explained by the Taylor expansion of the three absorption factors



$$A_S = \frac{\alpha}{4}, \quad (28)$$

$$A_E = \frac{-\log(1-\alpha)}{4} = \frac{1}{4}\alpha + \frac{1}{8}\alpha^2 + \frac{1}{12}\alpha^3 + \dots, \quad (29)$$

$$A_M = \frac{\alpha}{2(2-\alpha)} = \frac{1}{4}\alpha + \frac{1}{8}\alpha^2 + \frac{1}{16}\alpha^3 + \dots. \quad (30)$$

Note that the Eyring and modified absorption factors share their first two terms, and the Sabine absorption factor is the first order approximation of both of these. (That Sabine absorption coefficient is the first order approximation of the Eyring absorption coefficient is already well known in room acoustics.)

In addition, as the value of the absorption coefficient approaches one,  $A_E$  differs substantially from  $A_M$ :  $A_E$  increases unbounded while  $A_M$  maintains a finite value of 0.5. While the Eyring reverberation time equation<sup>16</sup> accounts reasonably well for the resulting infinitely short reverberation time, the Eyring-absorption factor  $A_E$  in the diffusion equation becomes singular. This is the failing point of the diffusion-Eyring model, which limits its applicability in often-encountered situations where walls, portions of walls, or opening in them have an absorption coefficient of 1.0.

### III. SIMULATIONS

In this section, three diffusion equation models (the diffusion equation with each of the three different boundary conditions) are compared to the geometrical-acoustic method implemented by a commercial software (CATT acoustics®) for three types of rooms: cubic rooms with both uniform and nonuniform absorption distribution, and a flat, long room, in terms of the RTs and SPLs. The diffusion equation models are solved by a commercially available finite element solver. The size of the mesh elements is chosen to be on the order of or smaller than one mean free path  $4V/S$  of the room.<sup>5</sup> The time step is chosen as 0.01 s for every case involving time-dependent calculations.

Equations (11) and (12) are solved for the initial condition

$$w(\mathbf{r}, 0) = 0 \quad \text{in } V, \quad (31)$$

$$w(\mathbf{r}, 0) = w_0 \quad \text{in } V_s, \quad (32)$$

where  $V_s$  is the volume occupied by the sound source.<sup>5</sup> With a time-dependent solution  $w(\mathbf{r}, t)$ , the sound energy-time function can be expressed as<sup>15,17</sup>

$$L_p(\mathbf{r}, t) = 10 \log \left( \frac{w(\mathbf{r}, t) \rho c^2}{P_{\text{ref}}^2} \right), \quad (33)$$

where  $P_{\text{ref}}$  equals  $2 \times 10^{-5}$  Pa. The sound energy decay functions as well as the RTs can then be obtained.

To calculate the steady state sound field, Eqs. (11) and (12) are solved for a given sound power  $W_s$  of the source, and then  $q(\mathbf{r}, t)$  is set to be equal to  $W_s/V_s$ . With a stationary

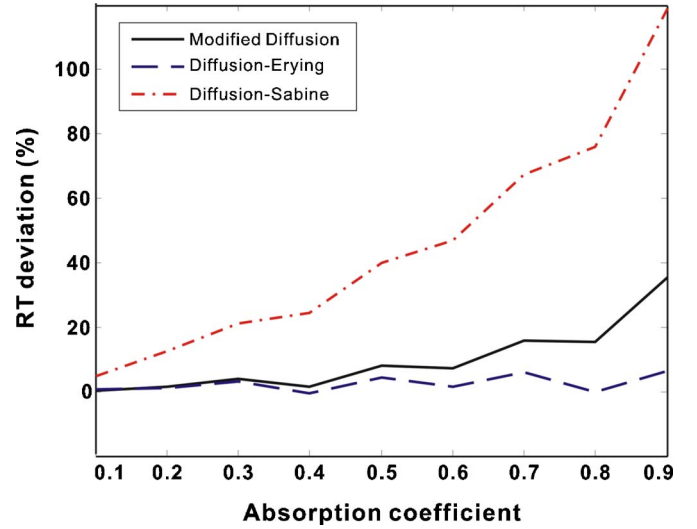


FIG. 3. (Color online). Deviations of the reverberation times calculated by the geometrical-acoustic model and three diffusion models.

solution  $w(\mathbf{r})$ , the total SPL  $L_p^{\text{tot}}(\mathbf{r})$ , including the direct field attributable to the point source, can be expressed as

$$L_p^{\text{tot}}(\mathbf{r}) = 10 \log \{ \rho c [W_s / (4\pi r^2) + w(\mathbf{r})c] / P_{\text{ref}}^2 \}. \quad (34)$$

#### A. Cubic rooms with uniformly distributed absorption coefficients

A cubic room with dimensions 5 m \* 5 m \* 5 m is modeled. The source is in the center of the room at coordinate (0, 0, 0) m. The absorption coefficient is assigned uniformly to all room surfaces and ranges from 0.1 to 0.9. The RTs are obtained at the position (1, 0, 0) by three diffusion equation models, and by the geometrical-acoustic model. The number of rays and the ray truncation time in CATT acoustics® are chosen as  $5 \times 10^4$  and 2000 ms, respectively, where the latter is much longer than the expected RT. The scattering coefficients on the walls are set at 100%, being compatible with the implicit requirement of the diffusion equation model, which is the configuration used throughout all simulations.

Figure 3 illustrates the difference, in terms of predicted RTs, between the results from the geometrical-acoustic model and those obtained via the other methods. Both the diffusion-Eyring and the modified diffusion model improve the simulation accuracy with respect to the diffusion-Sabine model, especially when the absorption coefficient is high. In addition, the diffusion-Eyring and modified diffusion models only show noticeable difference when the absorption coefficient exceeds approximately 0.6.

#### B. Cubic rooms with nonuniformly distributed absorption coefficients

The interior surfaces of another cubic room with the same dimensions are assigned two different absorption coefficients. One of the walls ( $x = -2.5$  m) is given an absorption coefficient of 1.0 while the other walls are assigned an absorption coefficient 0.5. The source is still in the center of the room at (0, 0, 0) m while the receivers are distributed along  $x = -2.5$  m to  $x = 2.5$  m, ( $y = z = 1$  m). The number of rays is

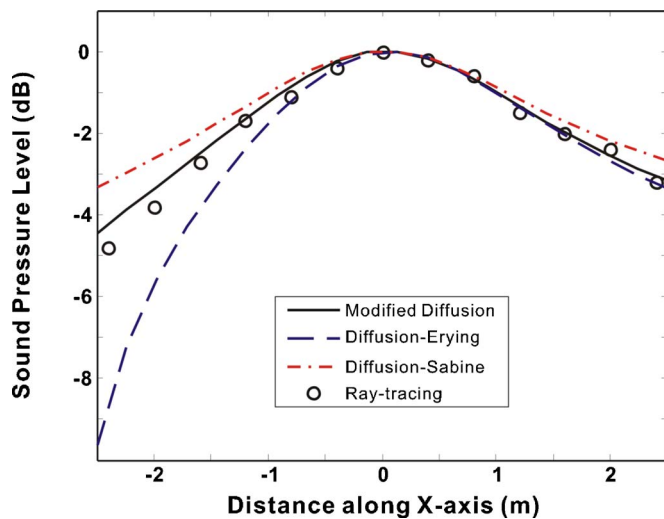


FIG. 4. (Color online). Comparison of sound pressure level distributions along  $y=z=1$  m in four different models of a cubic room with two different absorption coefficients, 1.0 and 0.5.

enlarged to  $1 \times 10^6$  and the truncation time is set to 2000 ms. The number of rays is much larger than in the last case because many rays are lost when they impinge upon the wall with  $\alpha=1.0$ . Using the diffusion-Eyring model, since one wall is featured with the absorption coefficient 1,  $-\log(1-\alpha)$  becomes an infinitely large value which cannot be implemented in the available finite element solver, thus, we use  $1e10$  instead of the infinitely large value. The results of SPLs shown in Fig. 4 indicate that:

1. The modified diffusion model predicts SPLs more accurately than does the diffusion-Sabine model.
2. When the room has one open side ( $\alpha=1.0$ ), the diffusion-Eyring model yields incorrect results, especially near the open side. The reverberant sound energy density is nearly zero at the open side calculated by the diffusion-Eyring model which is nonphysical. The very big value of  $1e10$  is used to represent the infinitely large value for the absorption term  $-\log(1-\alpha)$  in the simulations. Increasing this value towards infinity only causes it to deviate more from the results of the geometrical-acoustic model. Since the modified diffusion model does not have this singularity, it can realistically predict the sound field near highly absorptive boundaries.

When using CATT acoustics to obtain the correct late decay, the randomized tail-corrected cone-tracing method needs to extrapolate the reflection density growth (assuming it is quadratic) and is not accurate in an open room. Therefore, this work compares the predicted RTs by giving only the results of three diffusion equation models. In this case, three diffusion equation models have the following RTs at position (1 m, 1 m, 1 m): (diffusion-Sabine) 0.22 s, (diffusion-Eyring) 0.14 s, (modified diffusion) 0.19 s. Without any benchmark for comparison, no further conclusion is given at this time. However, an experiment involving open spaces is planned to provide the means for comparison and verification.

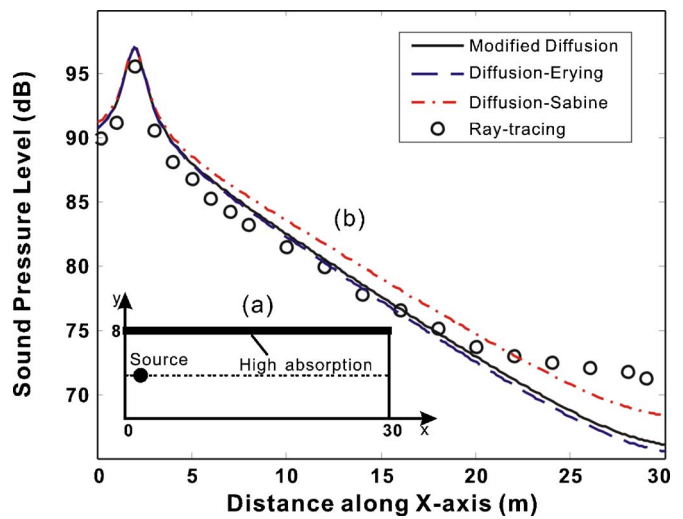


FIG. 5. (Color online). (a) Top view of a long, flat room with dimension  $30 \text{ m} \times 8 \text{ m} \times 3 \text{ m}$ , the sound source is at  $(2,4,2)$  m, the sound pressure levels are calculated along  $y=4$  m (dotted line). (b) Comparison of sound pressure level distributions along  $y=4$  m (dotted line) by four different models in a long, flat room with two different absorption coefficients, 0.8 and 0.2.

### C. Flat and long room

In this example, the three diffusion equation models are compared to the geometrical-acoustics model for a flat, and long room with dimensions  $30 \text{ m} \times 8 \text{ m} \times 3 \text{ m}$ . The source is located at  $(2,4,2)$  m, and the sound power level  $W_s$  is 100 dB. One side wall is assigned absorption coefficient 0.8, while the other five walls share absorption coefficient 0.2. Figure 5(a) illustrates a top view of this room.

Figure 5(b) illustrates the SPL distribution along the line  $y=4$  m ( $x$  is from 0 to 30 m) at height  $z=1.5$  m. In CATT acoustics® software the number of rays and the ray truncation time are chosen as  $5 \times 10^4$  and 2000 ms, respectively. Overall, the diffusion-Eyring model and the modified diffusion model agree better with the geometrical-acoustics model, although several points near the end of the room appear to be closer to the diffusion-Sabine model results.

## IV. EXPERIMENTAL VERIFICATION

This section describes acoustical measurements in a scale-model flat room to verify the diffusion equation model and further compare different boundary conditions for room-acoustic prediction in terms of SPL distributions and RTs. For a flat room, the sound energy density is known to be nonuniform. Statistical room-acoustic theory is unable to handle spatial distributions in highly irregular room shapes. This is the reason such a room was chosen for the experimental verification.

### A. Experimental setup

Physical scale modeling is a versatile research tool which has recently been applied in a variety of acoustic investigations.<sup>18-22</sup> In this study, a 1:8 scale model is used throughout the entire experiment. The dimensions of the scale model are  $1 \text{ m} \times 1 \text{ m} \times 0.2 \text{ m}$ , corresponding to  $8 \text{ m} \times 8 \text{ m} \times 1.6 \text{ m}$  in full scale. Hardwood along with one



FIG. 6. (Color online). Photograph of the flat room scale model showing the speaker, microphone, QRDs, foam, and rocks. A detailed photo of the scale-model sound source is shown in the left corner.

sheet of 5/4 in. plywood in thickness are used as wall materials to construct the room model. Diffusers on the walls are quadratic-residue diffusers (QRDs) and rocks, providing strong scattering at high frequency. In addition, such QRDs are known to be able to provide fairly good scattering for a wide range of frequencies. The QRDs are randomly distributed throughout the sidewalls (1.6 m high in full scale) of the scale model. The scattering frequency of the rocks will be discussed in the next section. In reality, diffuse reflections from the walls can be obtained even without such extensive treatment.<sup>23</sup> Two sidewalls near the sound source are of highly absorptive foam. Figure 6 shows a photograph of the scale model.

A 1/4 in. omni-directional microphone is used in the measurements. A miniature dodecahedron loudspeaker system is used as the sound source as shown in the left corner of Fig. 6. Measurements of directivities indicate that the dodecahedron loudspeaker system is omni directional in the frequency range of interest up to 32 kHz. Maximal-length sequence signals are used as an excitation signal. Room impulse responses are measured at chosen locations and the measurement procedure is controlled by a trigger mechanism throughout the entire measurement session to avoid any additional uncertainties across measurements. For frequency-dependent room-acoustic analysis the measured room impulse responses are filtered in octave bands. Figure 7 illustrates a segment of one of the room impulse responses, the corresponding energy-time function, and the Schroeder decay function at 1 kHz octave band.

The absorption coefficients of the materials are measured separately. Two proportionate scale-model rooms of which one is made of the rock-lined panels and the other is made of highly absorptive foam, are constructed and measured. The absorption coefficients of the rock panels and of the foam are estimated from the RTs by inverting the Eyring equation. To estimate the absorption coefficient of the QRD, all the foam in the scale model was first replaced by QRDs. Next, impulse responses are taken to obtain the RTs, and the absorption coefficient of the QRD is iteratively adjusted to

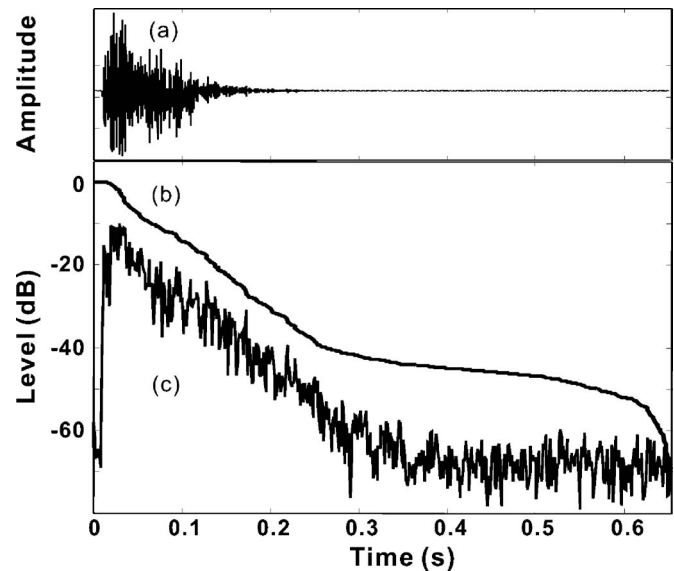


FIG. 7. Segment of one of the impulse responses, its energy-time curve, and its Schroeder decay function in the 1 kHz octave band. (a) Relative amplitude of the impulse response. (b) Schroeder decay curve. (c) Energy-time curve.

match predictions of RTs to experimental results.<sup>21</sup> Of the measured coefficients, that of the QRD is the primary uncertainty. However, the room-acoustic parameters in this case are determined primarily by the absorption coefficient of the rock panels simply because their areas are much greater than those of the QRDs or the foam in the scale model. Note that the scale model testing in this study is not to model a specific existing room, but rather for validation purpose, so no extra measures, such as nitrogen or drying air, are conducted for correcting air absorption in the scale model. However, all of the absorption coefficients of the scale-model wall materials are estimated from measurements made under normal atmospheric conditions. The excess air absorption is considered to be included in the estimated absorption coefficients of the wall materials. Table I lists the estimated absorption coefficients.

## B. Experimental verification of the diffusion equation model

The previous section compared the simulation results of three diffusion equation models with the geometrical-acoustic model. This section will compare experimental results from the scale-model flat room with the predictions of the diffusion equation model with the modified boundary condition.

Since the dimensions of the rocks are around 3–4 cm, they diffusely reflect the sound between 8.5 and 11.5 kHz,

TABLE I. Absorption coefficient of the materials used in the scale model at 1 and 2 kHz octave band (8 and 16 kHz octave band in the 1:8 scale model).

Material	1 kHz	2 kHz
QRD	0.10	0.05
Wooden panel with rocks	0.18	0.20
Foam	0.95	0.96



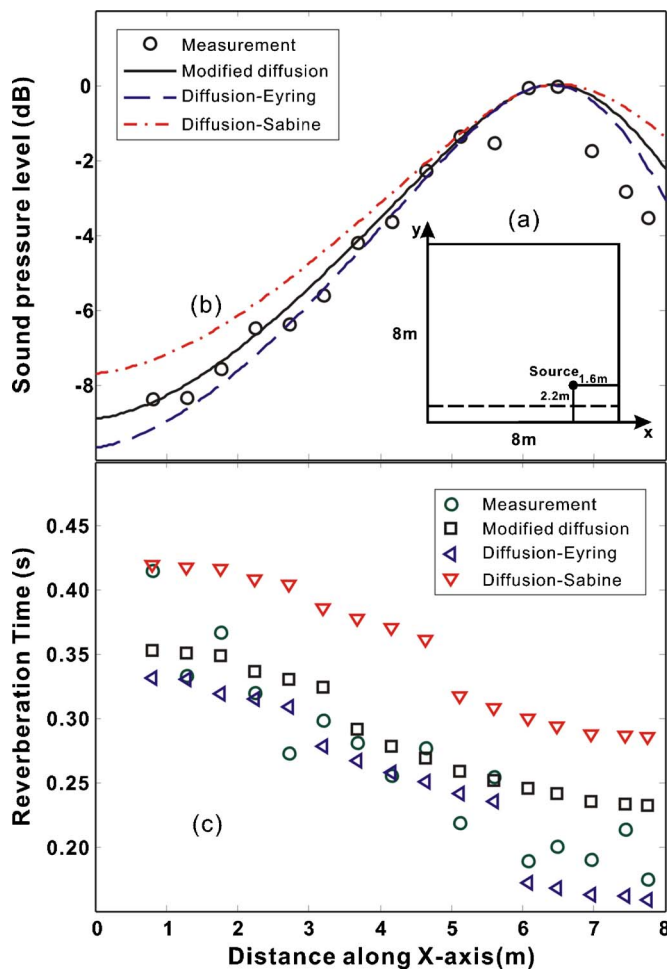


FIG. 8. (Color online). Comparison of three different diffusion models with experimental results in a scale-model flat room in the 1 kHz octave band along the line at  $y=0.64$  m (full scale). (a) A top-view of the flat room scale model. The source is located at the bottom right. The measurements are conducted along the dotted line. (b) Sound pressure level distributions. (c) Reverberation times.

which lies mostly within 1 kHz octave band (and partially in 2 kHz octave band) given the chosen scale factor 1:8. Therefore, the room boundaries meet the inherent requirement of the diffusion equation model best in the 1 kHz octave band, while they qualify only partially in the 2 kHz octave band. Therefore, this section will discuss only the results obtained in these two octave bands.

The measurements are conducted at 16 receiving points along a line near the source. Figure 8(a) illustrates a top view of the scale model. Figure 8(b) and Fig. 9(a) illustrate the SPLs measured in the scale-model flat room for 1 and 2 kHz octave bands, respectively. The SPLs are relative values which are referenced to the value predicted in simulation at  $x=6.4$  m (full scale), where all the diffusion equation models give the maximum value.

At 1 kHz, the diffusion-Eyring model and the modified diffusion model agree with the experimental results very well. The maximum deviation (2 dB) occurs near the foam, probably due to the fact that the foam is less diffusely reflecting. At 2 kHz, as shown in Fig. 9(a), although the diffusion-Sabine model shows better results for several points at the beginning, overall the diffusion-Eyring model

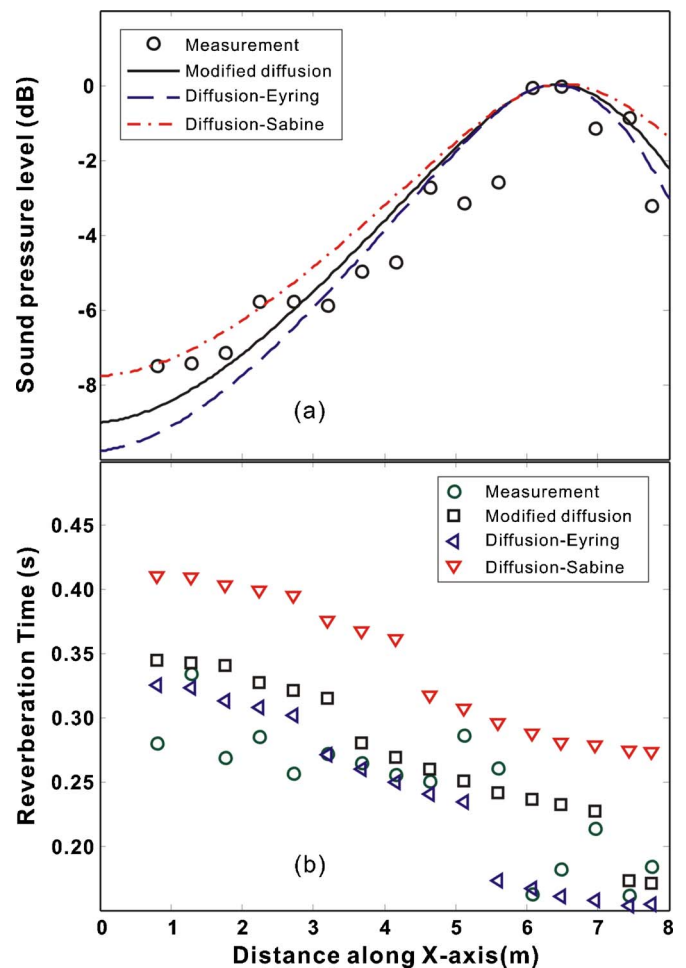


FIG. 9. (Color online). Comparison of three different diffusion models and experimental results in a scale-model flat room in the 2 kHz octave band along a line at  $y=0.64$  m (full scale). (a) Sound pressure level distributions. (b) Reverberation times.

and the modified diffusion model are closer to the experimental results. The worse agreement in comparison with those at 1 kHz should be expected, probably due to the lower degree of scattering of the rocks in this octave band.

At both 1 and 2 kHz, the original diffusion-Sabine model overestimates the RTs, while the diffusion-Eyring model and the modified diffusion model well predict the RTs as shown in Fig. 8(c) and Fig. 9(b). Moreover, the three diffusion equation models all predict the “drop” trend of the RT as the receiver location approaches the highly absorptive foam covered wall. The reason for this trend might be that the highly absorptive foam draws the energy much faster than the QRDs do. Note that the RTs predicted by the three diffusion equation models are not changed linearly along the almost linearly increasing  $x$ -axis distance. Some pronounced dips are found at different places for different diffusion equation models, while the experimental results also show several dips. For example, in Fig. 9(b), both experimental and the modified diffusion model results show a pronounced dip of the RT between  $x=7$  m and  $x=8$  m. No explanation for this has yet been found.

It seems plausible that the diffusion-Eyring model has slightly better agreement with the experimental results than



does the modified diffusion model for RT prediction. However, it is hard to conclude that in this specific case, the diffusion-Eyring model is more accurate at this moment, because of the uncertainty of the input parameter of the three diffusion equation models,<sup>21</sup> including absorption coefficients, directivities of the microphone and the loudspeaker, etc. Nevertheless, in extending this model to an uncovered room, the diffusion-Eyring model is expected to be problematic due to the singularity mentioned above. Such measurements should be done in the near future for further validations.

In the 250 and 500 Hz octave bands, the agreement between the predicted results and the experimental results in terms of SPLs and RTs drops markedly, due to the decreased diffuse reflections of the walls. It remains for future work to scrutinize the validity of each diffusion equation model with regard to different degrees of diffusion on the walls.

## V. CONCLUSION

This work introduces extensions of the diffusion equation model recently applied in room-acoustic predictions by proposing a modified boundary condition. A direct comparison of this modified boundary condition with two previous boundary conditions: diffusion-Sabine and diffusion-Eyring boundary conditions, suggests that these three boundary conditions behave similarly in low absorption region while a considerable discrepancy will be seen in high absorption region. Particularly, there exists a singularity within the diffusion-Eyring model when the absorption coefficient becomes 1.0. The diffusion equation model using the modified boundary condition overcomes the singularity problem. To further compare them, a geometrical-acoustic model is employed as a reference, with RTs and SPLs investigated in cubic rooms. For uniformly distributed absorption coefficients, both the diffusion-Eyring model and the modified diffusion model show good agreement with the geometrical-acoustic model. For nonuniformly distributed absorption coefficients, if the wall has one side open or an absorption coefficient of 1.0, the diffusion-Eyring model fails. Simulations of sound pressure levels (SPLs) in a long, flat room with an average absorption coefficient below 0.8, indicate that the diffusion-Eyring and the modified diffusion model yield very similar results being closer to those estimated by the geometrical-acoustics method.

The experimental results obtained from a scale-model flat room are discussed to further examine the modified diffusion model. Both SPL and RT distributions indicate that the diffusion equation model is capable of modeling the sound field in disproportionate rooms for the nonuniformity of sound energy density as well as the sound energy decay. Within frequency ranges where diffuse surface reflections can be achieved in the scale model, the modified diffusion model and the diffusion-Eyring model agree well with the scale-model experimental results.

The diffusion-Eyring and the modified diffusion model both exceed the diffusion-Sabine model in terms of room-acoustic prediction accuracy. The modified diffusion model provides comparable results with the diffusion-Eyring model in most cases investigated within this study. More impor-

tantly, the modified diffusion model can handle an absorption coefficient as high as 1.0, while the diffusion-Eyring model fails due to the singularity.

The discussion of the illustrative examples is limited so far to the cases where the numerical simulations and, particularly the experimental verifications, are conducted using a flat room scale model. More systematic investigations using other room types, including long room scale models, real-size rooms, and coupled spaces, are expected in the near future.

## ACKNOWLEDGMENTS

The authors would like to thank Dr. Bengt-Inge Dalenbäck, Dr. Edward W. Larsen, and Professor Paul Calamia for useful discussions. They also thank Aaron Catlin and Xiaohu Chen for their help during the acoustic measurement and Stephen Olson for a critical review of the final draft.

- <sup>1</sup>F. Ollendorff, "Statistical room-acoustics as a problem of diffusion (a proposal)," *Acustica* **21**, 236–245 (1969).
- <sup>2</sup>P. M. Morse and H. Feshbach, *Methods of Theoretical Physics* (McGraw-Hill, New York, 1953).
- <sup>3</sup>J. Picaut, L. Simon, and J. D. Polack, "A mathematical model of diffuse sound field based on a diffusion equation," *Acustica* **83**, 614–621 (1997).
- <sup>4</sup>V. Valeau, M. Hodgson, and J. Picaut, "A diffusion-based analogy for the prediction of sound fields in fitted rooms," *Acustica* **93**, 94–105 (2007).
- <sup>5</sup>V. Valeau, J. Picaut, and M. Hodgson, "On the use of a diffusion equation for room-acoustic prediction," *J. Acoust. Soc. Am.* **119**, 1504–1513 (2006).
- <sup>6</sup>J. Picaut, L. Simon, and J. Hardy, "Sound field modeling in streets with a diffusion equation," *J. Acoust. Soc. Am.* **106**, 2638–2645 (1999).
- <sup>7</sup>J. Picaut, L. Simon, and J. D. Polack, "Sound field in long rooms with diffusely reflecting boundaries," *Appl. Acoust.* **56**, 217–240 (1999).
- <sup>8</sup>A. Billon, V. Valeau, A. Sakout, and J. Picaut, "On the use of a diffusion model for acoustically coupled rooms," *J. Acoust. Soc. Am.* **120**, 2043–2054 (2006).
- <sup>9</sup>Y. Jing and N. Xiang, "A modified diffusion equation for room-acoustic prediction (L)," *J. Acoust. Soc. Am.* **121**, 3284–3287 (2007).
- <sup>10</sup>A. Billon, J. Picaut, and A. Sakout, "Prediction of the reverberation time in high absorbent room using a modified-diffusion model," *Appl. Acoust.* **69**, 68–74 (2008).
- <sup>11</sup>R. C. Haskell, L. O. Svaasand, T. Tsay, T. Feng, M. S. McAdams, and B. J. Tromberg, "Boundary conditions for the diffusion equation in radiative transfer," *J. Opt. Soc. Am. A* **11**, 2727–2741 (1994).
- <sup>12</sup>W. B. Joyce, "Classical-particle description of photons and phonons," *Phys. Rev. D* **9**, 3234–3256 (1974).
- <sup>13</sup>J. Picaut, A. Billon, V. Valeau, and A. Sakout, "Sound field modeling in architectural acoustics using a diffusion equation," *Proc. Inter-Noise* 2006.
- <sup>14</sup>U. J. Kurze, "Scattering of sound in industrial spaces," *J. Sound Vib.* **98**, 349–364 (1985).
- <sup>15</sup>A. D. Pierce, *Acoustics: An Introduction to Its Physical Principles and Applications* (Acoustical Society of America, Melville, New York, 1981).
- <sup>16</sup>H. Kuttruff, *Room Acoustics* 4th ed. (Spon, New York, 2000).
- <sup>17</sup>M. R. Schroeder, "New method of measuring reverberation time," *J. Acoust. Soc. Am.* **37**, 409–412 (1965).
- <sup>18</sup>W. Yang and M. Hodgson, "Ceiling baffles and reflectors for controlling lecture-room sound for speech intelligibility," *J. Acoust. Soc. Am.* **121**, 3517–3526 (2007).
- <sup>19</sup>N. Xiang and J. Blauert, "Binaural scale modeling for auralisation and prediction of acoustics in auditoria," *Appl. Acoust.* **38**, 267–290 (1993).
- <sup>20</sup>K. M. Li and K. K. Lu, "Evaluation of sound in long enclosures," *J. Acoust. Soc. Am.* **116**, 2759–2770 (2007).
- <sup>21</sup>J. E. Summers, R. R. Torres, Y. Shimizu, and B. L. Dalenback, "Adapting a randomized beam-axis-tracing algorithm to modeling of coupled rooms via late-part ray tracing," *J. Acoust. Soc. Am.* **118**, 1491–1502 (2005).
- <sup>22</sup>J. Jeon and M. Barron, "Evaluation of stage acoustics in Seoul Arts Center Concert Hall by measuring stage support," *J. Acoust. Soc. Am.* **117**, 232–239 (2005).
- <sup>23</sup>M. Hodgson, "Evidence of diffuse surface reflections in rooms," *J. Acoust. Soc. Am.* **89**, 765–771 (1991).